Journal of Sound and Vibration 325 (2009) 649–663

Contents lists available at ScienceDirect

Journal of Sound and Vibration

journal homepage: www.elsevier.com/locate/jsvi

On the effects of reflections on time delay estimation for leak detection in buried plastic water pipes

Y. Gao, M.J. Brennan *, P.F. Joseph

Institute of Sound and Vibration Research, University of Southampton, Southampton SO17 1BJ, UK

ARTICLE INFO

Article history:
Received 19 October 2008
Received in revised form
21 March 2009
Accepted 24 March 2009
Handling Editor: K. Shin
Available online 8 May 2009

ABSTRACT

This paper is concerned with the way in which wave reflections in a fluid-filled pipe affect the cross-correlation function of two leak noise signals used to detect and locate leaks in buried water pipes. Propagating waves generated by leak noise reverberate in a pipe network system, as they encounter features such as changes in section, and resistance such as valves, and pipe junctions. A theoretical model of a straight pipe with discontinuities, which cause reflections, is developed and incorporated into a model of the cross-correlation function. The reasons why the reflections and the low-pass filtering properties of the pipe can be largely removed by the generalised cross-correlation (GCC) phase transform (PHAT) are determined. Using the analytical model, theoretical predictions of the basic cross-correlation function (BCC) and the GCC PHAT are compared with experimental data from a specially constructed test site in Canada.

1. Introduction

A leak from a water supply pipe system generally generates noise, which can be used to detect and locate the leak. To achieve this the basic cross-correlation (BCC) technique is commonly used to estimate the time delay between two acoustic/vibration signals measured either side of the leak [1–3]. Although useful in many practical situations, it has proved to be problematic in plastic pipes, since the acoustic signals in these pipes are heavily attenuated, generally narrow-band and of low frequency [4,5].

Gao et al. [6] has investigated this phenomenon by incorporating an analytical model of wave propagation in water-filled plastic pipes into the cross-correlation function. They subsequently used this model to examine a range of cross-correlation methods (generalised cross-correlation (GCC) functions) for leak detection [7], first investigated by Knapp and Carter [8]. However, they assumed that the pipe was infinite in length, i.e., no reflections occurred in the pipe, which is often not the case in practice. Frequently, waves generated by a leak reverberate around the pipe network due to features such as changes in section, and the presence of valves and pipe junctions [9]. As a result, waves incident on these features can experience reflection (some energy of the wave is reflected), absorption (the amplitude of the wave is attenuated) and transmission (the wave is transmitted past the feature). The presence of reflections are highly undesirable from the perspective of leak detection, as they introduce peaks in the cross-correlation function in addition to the peak corresponding to the true time delay resulting from the propagating leak noise. This sometimes makes it difficult to interpret the cross-correlation function as demonstrated in this paper.

* Corresponding author. Tel.: +44 23 8059 3756; fax: +44 23 8059 3190.
E-mail address: mjb@isvr.soton.ac.uk (M.J. Brennan).

0022-460X/$ - see front matter © 2009 Elsevier Ltd. All rights reserved.
doi:10.1016/j.jsv.2009.03.037

Previous work by the authors [7] has shown that GCC methods offer a potential improvement over the BCC method in the application of water leak detection. For example, the analytical model of the cross-correlation function of leak signals in plastic pipes developed by Gao et al. [7,10] shows that a plastic pipe essentially acts as an acoustic low-pass filter, which degrades the estimation of the time delay. The filtering properties of the pipe can, to some extent, be compensated for by pre-whitening the signals prior to calculating the cross-correlation function. For instance, the PHAT method "flattens" the modulus of the CSD spectrum and thus effectively only transforms the phase of the CSD spectrum between the leak signals measured at two locations into the time domain cross-correlation function [7]. In the absence of reflections, the phase spectrum has a constant gradient, so the corresponding correlation function for signals with infinite frequency bandwidth is a delta function. In practical situations, however, the estimate of the actual time delay is corrupted due to the existence of background noise and the filtering effect of the pipe on the phase spectrum.

The entire process of wave propagation in pipes can be modelled using various simulation approaches, including the method of characteristics [11,12], bond graph modelling [13], modal analysis [14] and the transmission modelling technique [15–17]. Although these methods are commonly used to model waves in pipeline networks, in this paper an approach using transmission and reflection coefficients is used to model discontinuities in the pipe.

The aim of this paper is to quantify the effects of reflections in a water-filled pipe on the cross-correlation function. It builds on previous work by the authors, which assumed that the pipe was infinitely long so that reflections do not occur. In this work a more realistic model is used, which includes reflections and then shows how the reflections affect the cross-correlation function. The paper then proceeds to examine the use of the GCC phase transform (GCC PHAT) as a means of suppressing the additional peaks in the cross-correlation function.

To illustrate the effect of reflections on the cross-correlation function, analysis is carried out for the simple case of a pipe with two discontinuities. The effect of reflections on time delay estimation is studied for both the basic cross-correlation (BCC) and the GCC PHAT. Theoretical predictions, based on a simple pipe model with reflections, are compared to the BCC and GCC PHAT calculated from test data obtained from buried PVC water pipes.

2. Overview of leak detection using cross-correlation methods

The authors have published several papers on leak detection in buried plastic pipes [6,7,10,18] using acoustic methods, and the reader is referred to these for detailed information on the general principles of leak detection and the factors which affect it. In this section only a brief overview is given. Any reflections due to discontinuities in the pipe are initially considered to be negligible.

To determine the position of a leak in water distribution pipes, vibration or acoustic signals are measured at two access points using sensors such as accelerometers or hydrophones, either side of the location of a suspected leak, as shown in Fig. 1. If a leak exists, a distinct peak may be found in the cross-correlation of the two signals $x_1(t)$ and $x_2(t)$. This gives an estimate of the time delay T_0 that corresponds to the difference in arrival times between the leak signals at each sensor. The relationship between the time delay and the distances d_1 and d_2 between the leak and the sensors is given by

$$T_0 = \frac{d_1 - d_2}{c}, \tag{1}$$

where c is propagation speed of the leak noise in the buried pipe. The time delay is determined by calculating the time at which the weighted cross-correlation function of the leak noise signals given by [6]

$$R^g_{x_1x_2}(\tau) = F^{-1}\{\Psi_g(\omega)S_{x_1x_2}(\omega)\} = \frac{1}{2\pi}\int_{-\infty}^{+\infty} \Psi_g(\omega)S_{x_1x_2}(\omega)e^{i\omega\tau}\,d\omega, \tag{2}$$

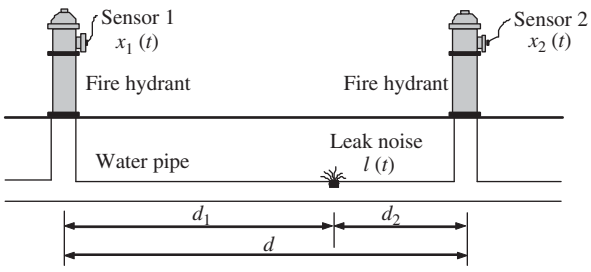

Fig. 1. Schematic of a pipe with a leak bracketed by two sensors.

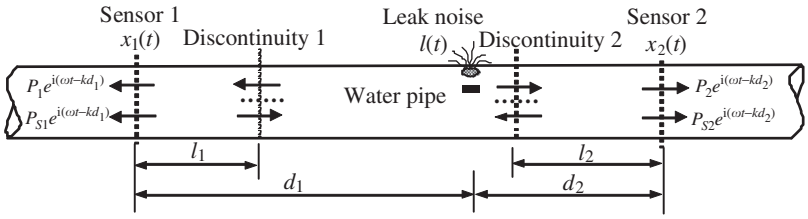

Fig. 2. Wave propagation and reflection in a pipe with two in-bracket discontinuities.

is a maximum, where $F^{-1}\{\cdot\}$ denotes the inverse Fourier transform; $S_{x_1x_2}(\omega)$ is the cross-spectral density (CSD) between the measured acoustic signals, $\Psi_g(\omega)$ is the weighting function that depends on the type of correlator employed and ω is circular frequency. The effects of several different weighting functions on the cross-correlation function, in the context of leak detection, have been discussed in Ref. [7]. When $\Psi_g(\omega)=1$, the GCC methods all reduce to the BCC method. In practice, only an estimate of the cross-correlation function can be obtained since it is derived from finite time observations of $x_1(t)$ and $x_2(t)$.

3. A model of the cross-correlation function including wave reflections

To investigate the effect of reflections on the correlation technique, two discontinuities are considered, at distances l_1 and l_2 from the sensors, as shown in Fig. 2. Although the case considered here consists of discontinuities between the leak and the sensor (in-bracket discontinuities), the conclusions drawn are also applicable to out-of-bracket discontinuities. At each sensor location d_1 and d_2, there are two types of propagating/reflected waves including the primary propagating/reflected waves and subsequent secondary propagating/reflected waves. The pipe is assumed to be of infinite length, and the acoustic pressure can be considered to be uniform across the cross-section and is given by [7]

$$p(x)=P_0(\omega)\mathrm{e}^{-\mathrm{i}kx}, \tag{3}$$

where x is the distance between the leak and sensor signals; $P_0(\omega)$ is the amplitude of the acoustic pressure at the leak location at $x=0$ and $k=\omega/c(1-i\eta/2)$ where η is the loss factor in the buried pipe and c is the wave speed. In the frequency domain, the primary propagating/reflected waves are $P_1\mathrm{e}^{-\mathrm{i}kd_1}$ at distance d_1 and $P_2\mathrm{e}^{-\mathrm{i}kd_2}$ at distance d_2, where

$$P_1\mathrm{e}^{-\mathrm{i}kd_1}=t_1P_0(\omega)\mathrm{e}^{-\mathrm{i}kd_1}+r_2t_1P_0(\omega)\mathrm{e}^{-\mathrm{i}k(d_1+2d_2-2l_2)} \tag{4}$$

and

$$P_2\mathrm{e}^{-\mathrm{i}kd_2}=t_2P_0(\omega)\mathrm{e}^{-\mathrm{i}kd_2}+r_1t_2P_0(\omega)\mathrm{e}^{-\mathrm{i}k(d_2+2d_1-2l_1)}, \tag{5}$$

respectively. Here t_1 and t_2 are pressure transmission coefficients, and r_1 and r_2 are pressure reflection coefficients at discontinuities 1 and 2, respectively, which can be complex and frequency dependent. The subsequent secondary propagating/reflected waves $P_{s_1}\mathrm{e}^{-\mathrm{i}kd_1}$ at distance d_1 and $P_{s_2}\mathrm{e}^{-\mathrm{i}kd_2}$ at distance d_2 are determined by the repeated multiplication of these terms by $r_1r_2\mathrm{e}^{-\mathrm{i}k2(d-l)}$, where $d=d_1+d_2$ and $l=l_1+l_2$.

The total acoustic pressure at distances d_1 and d_2 can be obtained by repeating this process indefinitely, and is thus given by

$$p(\omega,d_1)=P_1\mathrm{e}^{-\mathrm{i}kd_1}+P_{s_1}\mathrm{e}^{-\mathrm{i}kd_1}=t_1P_0(\omega)\mathrm{e}^{-\mathrm{i}kd_1}\{1+r_2\mathrm{e}^{-\mathrm{i}k2(d_2-l_2)}\}\sum_{n=0}^{\infty}(r_1r_2)^n\mathrm{e}^{-\mathrm{i}k2n(d-l)}, \tag{6}$$

and

$$p(\omega,d_2)=P_2\mathrm{e}^{-\mathrm{i}kd_2}+P_{s_2}\mathrm{e}^{-\mathrm{i}kd_2}=t_2P_0(\omega)\mathrm{e}^{-\mathrm{i}kd_2}\{1+r_1\mathrm{e}^{-\mathrm{i}k2(d_1-l_1)}\}\sum_{n=0}^{\infty}(r_1r_2)^n\mathrm{e}^{-\mathrm{i}k2n(d-l)}, \tag{7}$$

respectively. From Eq. (6), the frequency response function $H(\omega,d_1)$ between the leak and sensor signal 1 is given by

$$H(\omega,d_1)=\frac{p(\omega,d_1)}{P_0(\omega)}=t_1\mathrm{e}^{-\mathrm{i}kd_1}\{1+r_2\mathrm{e}^{-\mathrm{i}k2(d_2-l_2)}\}\sum_{n=0}^{\infty}(r_1r_2)^n\mathrm{e}^{-\mathrm{i}k2n(d-l)}. \tag{8}$$

Since $|r_1r_2\mathrm{e}^{-\mathrm{i}k2(d-l)}|<1$, the summation of the series $\sum_{n=0}^{\infty}(r_1r_2)^n\mathrm{e}^{-\mathrm{i}k2n(d-l)}$ is given by

$$\sum_{n=0}^{\infty}(r_1r_2)^n\mathrm{e}^{-\mathrm{i}k2n(d-l)}=\frac{1}{1-r_1r_2\mathrm{e}^{-\mathrm{i}k2(d-l)}}. \tag{9}$$

Therefore, Eq. (8) can be written as

$$H(\omega,d_1)=\frac{t_1e^{-ikd_1}\{1+r_2e^{-ik2(d_2-l_2)}\}}{1-r_1r_2e^{-ik2(d-l)}}. \tag{10}$$

Similarly the frequency response function $H(\omega,d_2)$ between the leak and sensor signal 2 is given by

$$H(\omega,d_2)=\frac{t_2e^{-ikd_2}\{1+r_1e^{-ik2(d_1-l_1)}\}}{1-r_1r_2e^{-ik2(d-l)}}. \tag{11}$$

For two signals $x_1(t)$ and $x_2(t)$ measured at positions $x=d_1$ and d_2, the CSD $S_{x_1x_2}(\omega)$ is given by

$$S_{x_1x_2}(\omega)=H^*(\omega,d_1)H(\omega,d_2)S_{ll}(\omega), \tag{12}$$

where * denotes conjugation; $S_{ll}(\omega)$ is the auto-spectral density (ASD) of the acoustic pressure generated by the leak signal $l(t)$ measured at the leak location.

Substituting the frequency response functions $H(\omega,d_1)$ and $H(\omega,d_2)$ given by Eqs. (10) and (11) into Eq. (12) gives

$$S_{x_1x_2}(\omega)=\frac{t_1t_2S_{ll}(\omega)C(\omega)}{B(\omega)}|A(\omega)|e^{i(\omega T_0+\phi(\omega))}, \tag{13}$$

where

$$T_0=(d_1-d_2)/c;$$

$$|A(\omega)|e^{j\phi(\omega)}=1+r_1e^{-i\omega2(d_1-l_1)/c}e^{-\omega\eta(d_1-l_1)/c}+r_2e^{i\omega2(d_2-l_2)/c}e^{-\omega\eta(d_2-l_2)/c}+r_1r_2e^{i\omega2(\Delta d-\Delta l)/c}e^{-\omega\eta(d-l)/c},$$

$$B(\omega)=|1-r_1r_2e^{-i\omega2(d-l)/c}e^{-\omega\eta2(d-l)/c}|^2,$$

and

$$C(\omega)=e^{-\omega\eta(d_2+d_1)/2c}.$$

Here $\Delta d=d_2-d_1$ and $\Delta l=l_2-l_1$. Since multiplication in one domain is a convolution in the transformed domain, the cross-correlation function $R_{x_1x_2}(\tau)$ is given by

$$R_{x_1x_2}(\tau)=F^{-1}\{S_{x_1x_2}(\omega)\}=t_1t_2R_{ll}(\tau)\otimes c(\tau)\otimes b^{-1}(\tau)\otimes a(\tau)\otimes\delta(\tau+T_0), \tag{14}$$

where $\otimes$ denotes convolution; $R_{ll}(\tau)=F^{-1}\{S_{ll}(\omega)\}$ is the auto-correlation function of the leak signal;. $c(\tau)=F^{-1}\{C(\omega)\}$; $b^{-1}(\tau)=F^{-1}\{1/B(\omega)\}$; $a(\tau)=F^{-1}\{A(\omega)\}$; $\delta(\tau)$ is the Dirac delta function. The corresponding phase spectrum that is related to the time shift experienced by the signals as they propagate along the pipe, is given by

$$\Phi_{x_1x_2}(\omega)=\arg\{S_{x_1x_2}(\omega)\}=\omega T_0+\phi(\omega). \tag{15}$$

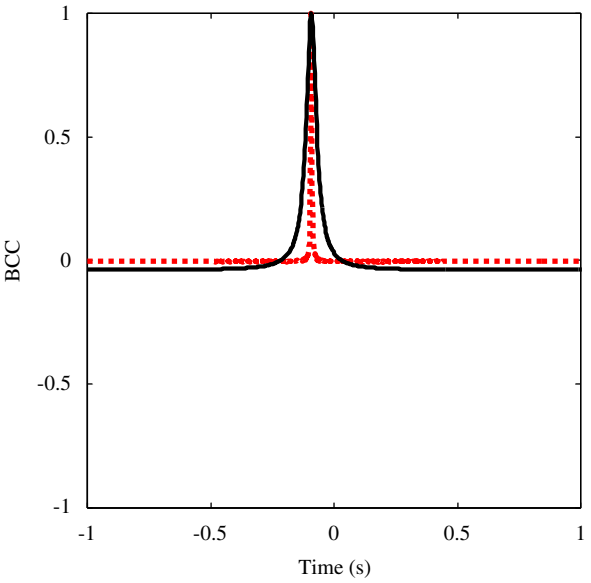

Fig. 3. The BCC function of the two pressure signals normalised to the maximum value, with a frequency bandwidth of 0–250 Hz. Solid black line: $\eta=0.22$ and dotted red line: $\eta=0.022$. There are no discontinuities in the pipe: $d_1=76.7$ m, $d_2=32.8$ m and $c=479\,\mathrm{ms}^{-1}$. (For interpretation of the references to colour in this figure legend, the reader is referred to the web version of this article.)

Note that the term $\phi(\omega)$ is generally a nonlinear function of frequency so that the presence of reflections, as described by the term $A(\omega)$, causes the phase spectrum to deviate from the linear phase spectrum ωT_0 that would be present if reflections were absent.

4. Effects of reflections on the cross-correlation function

Before considering the effects of reflections it is helpful to review the filtering effects of the pipe and the effects of any band pass filtering on the cross-correlation function. It has been shown in previous work [7] that there is a peak in the cross correlation function corresponding to the time delay resulting from the propagating leak signals despite the spreading phenomenon caused by the leak spectrum and the nature of wave propagation along the pipes. This is demonstrated in Fig. 3, which shows the difference in the basic cross-correlation function, for a high level of damping in the pipe of $\eta = 0.22$ and a relatively low damping level of $\eta = 0.022$, in an infinite pipe. The first of these values was chosen as it corresponds to the loss factor used in Ref. [6], and the second value was chosen as it is an order of magnitude less, and

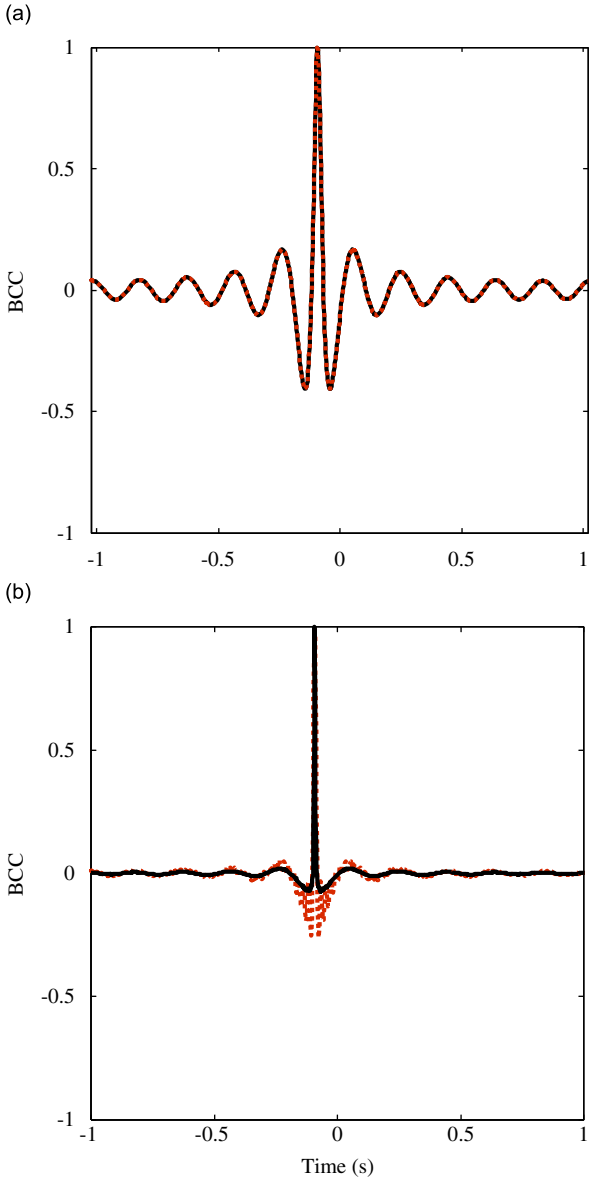

Fig. 4. The BCC function of the two pressure signals normalised to the maximum value. (a) $\eta = 0.22$ and (b) $\eta = 0.022$. Solid black line: frequency bandwidth of 5–250 Hz and dashed red line: frequency bandwidth of 5–50 Hz. There are no discontinuities in the pipe: $d_1 = 76.7$ m, $d_2 = 32.8$ m and $c = 479\,\mathrm{ms}^{-1}$. (For interpretation of the references to colour in this figure legend, the reader is referred to the web version of this article.)

represents relatively light damping. The distances chosen for the simulation of $d_1 = 76.7$ m, $d_2 = 32.8$ m and wave speed $c = 479\,\mathrm{ms}^{-1}$ also correspond to the values used in Ref. [6] and are related to the experimental work discussed later in this paper. Fig. 4 demonstrates the effect of band pass filtering the signals prior to calculating the cross-correlation function. It can be seen that the effect of band-pass filtering is to introduce a ripple into the cross-correlation function, but the degree of ripple is dependent on the damping in the pipe and the bandwidth. Damping in the pipe-wall causes the leak noise to attenuate with both distance and frequency. The attenuation in dB/m along the pipe is given by [19]

$$\text{Attenuation (dB/m)} = \frac{20(\omega\eta/2c)}{\ln(10)}. \tag{16}$$

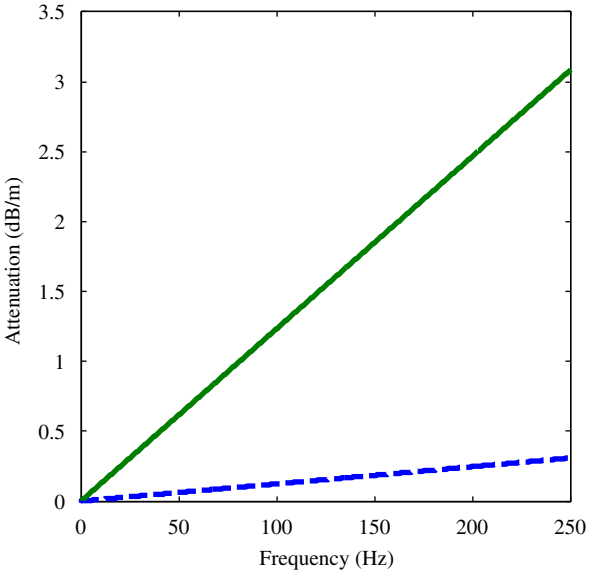

Fig. 5. Attenuation of leak noise along the pipe as a function of frequency, $c = 479\,\mathrm{ms}^{-1}$. Solid green line: $\eta = 0.22$ and dashed blue line: $\eta = 0.022$. (For interpretation of the references to colour in this figure legend, the reader is referred to the web version of this article.)

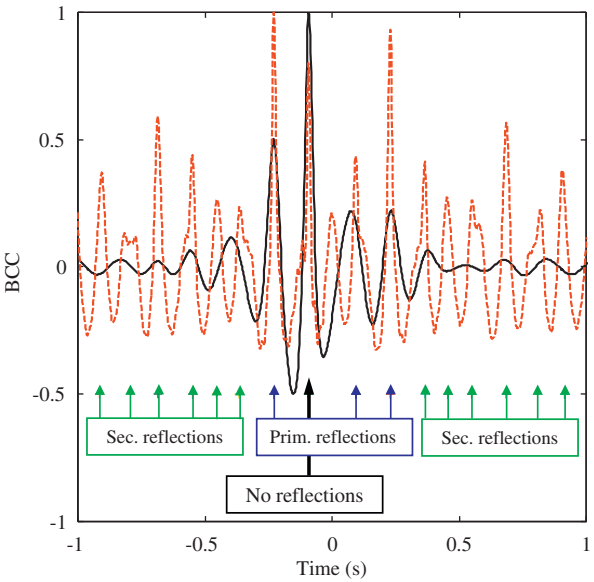

Fig. 6. The BCC function of the two pressure signals in the frequency range 5–250 Hz normalised to the maximum value for a pipe with reflecting terminations at the sensor positions. Solid black line: $\eta = 0.22$ and dashed red line: $\eta = 0.022$: $d_1 = 76.7$ m, $d_2 = 32.8$ m and $c = 479\,\mathrm{m\,s}^{-1}$ $l_1 = l_2 = 0$, $r_1 = r_2 = 1$. Primary reflections are given by $A(\omega)$ and the secondary reflections by $B(\omega)$ in Eq. (13). (For interpretation of the references to colour in this figure legend, the reader is referred to the web version of this article.)

This is plotted in Fig. 5 for two values of the loss factor, $\eta = 0.22$ and 0.022. It can be seen that the loss factor has a significant influence on the attenuation of the leak noise. For example, when the loss factor is $\eta = 0.22$, at 250 Hz the attenuation at $d_1 = 76.7$ m is 237 dB and at $d_2 = 32.8$ m it is 101 dB; at a frequency of 50 Hz the attenuation is 47 dB at $d_1 = 76.7$ m and 20 dB at $d_2 = 32.8$ m. Thus, when the damping in the pipe is high, $\eta = 0.22$, the upper cut-off frequencies of 50 and 250 Hz have a negligible effect on the BCC shown in Fig. 4a. When the loss factor is relatively low, $\eta = 0.022$, at a frequency of 250 Hz the attenuation is about 24 and 10 dB at d_1 and d_2, respectively. At a frequency of 50 Hz this changes to about 5 and 2 dB at d_1 and d_2, respectively. Thus, when the damping is lower, $\eta = 0.022$, the high frequency cut-off values of 50 and 250 Hz for the band pass filter have some effect as shown in Fig. 4b.

When reflections occur, the cross-correlation function changes further. This is caused by the existence of the primary propagating/reflected waves given by $A(\omega)$ and subsequent secondary propagating/reflected waves represented by $B(\omega)$ in Eq. (13). The level of contributions of the spurious peaks to the correlation function depends on the magnitude of the reflections r_1, r_2, and the locations of the sensors and discontinuities. The effect of reflections on the cross-correlation function is complicated, since both the modulus and phase spectra are affected by the discontinuities. For two values of damping, $\eta = 0.22$ and 0.022, and for lossless, reflecting discontinuities at the sensor positions, the BCC function is plotted

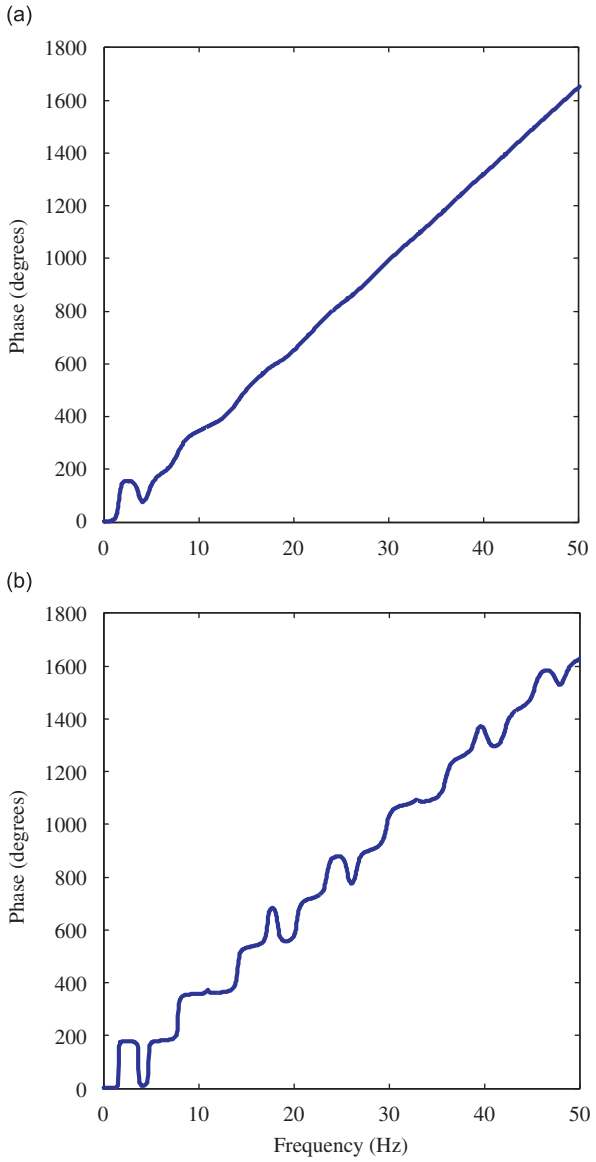

Fig. 7. Unwrapped phase of the cross-spectrum of the two pressure signals corresponding to the cross-correlation function shown in Fig. 6: (a) $\eta = 0.22$ and (b) $\eta = 0.022$. $d_1 = 76.7$ m, $d_2 = 32.8$ m and $c = 479\,\mathrm{m\,s^{-1}}$, $l_1 = l_2 = 0$, $r_1 = r_2 = 1$.

in Fig. 6. The peak due to the leak noise, which occurs because of wave propagation with no reflections at $\tau = -T_0$, is marked in the figure as are the peaks due to the primary reflections ($\tau = -T_0 + 2(d_1 - l_1)/c$, $\tau = -T_0 - 2(d_2 - l_2)/c$ and $\tau = -T_0 - 2(\Delta d - \Delta l)/c$) and secondary reflections. It can be seen that when damping is light (or if the measurement positions and discontinuities are close to the leak), the primary reflections result in a BCC which is difficult to interpret with respect to leak detection.

It has been shown by the authors [7] that the PHAT GCC function is effective in suppressing the additional peaks that are found in the BCC. In the remainder of this paper the reason why this is so is investigated. In Ref. [18] the relationship between the cross-spectrum and the time delay estimated by the cross-correlation function was determined. It was shown that the BCC effectively minimises the weighted mean square error between the estimated phase and the actual phase corresponding to the true time delay, where the weighting function is the modulus of the CSD. The way in which the damping affects the unwrapped phase of the CSD is shown in Fig. 7, which corresponds to the pipe system analysed in Fig. 6. The deviations from a straight line are due to reflections. It can be seen that in the highly damped case, $\eta = 0.22$, phase deviations are only prominent at low frequencies, and when the damping is higher, $\eta = 0.022$, the deviations are more pronounced and appear over a wider frequency range, due to the reflections. As well as these deviations in phase (from

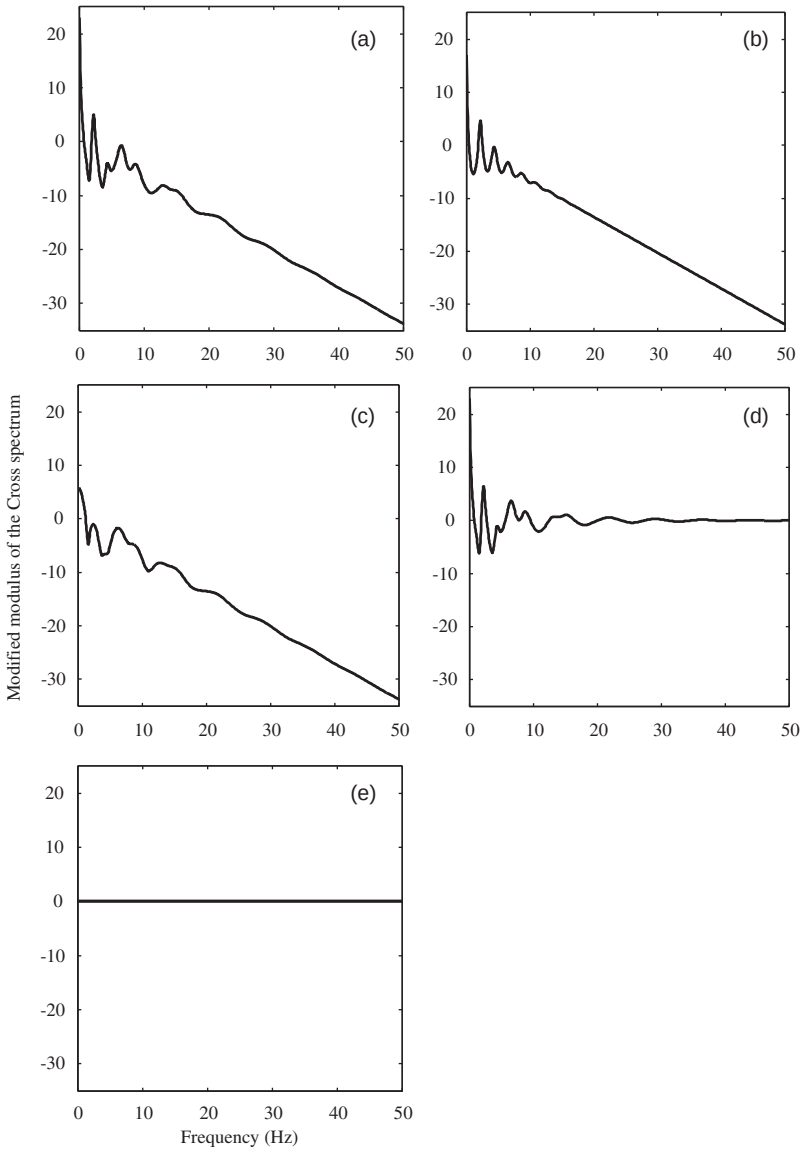

Fig. 8. Modified modulus of the cross-spectrum of the pressure signals corresponding to the phase spectrum in Fig. 7(a); $\eta = 0.22$, $d_1 = 76.7$ m, $d_2 = 32.8$ m, $c = 479\,\mathrm{ms}^{-1}$, $l_1 = l_2 = 0$, $r_1 = r_2 = 1$. (a) BCC, (b) primary reflections removed, (c) secondary reflections removed, (d) filtering effect of pipe removed, (e) divided by the modulus of the cross-spectrum.

that due directly from the leak noise (no reflections), the modulus of the CSD is also affected, as mentioned above. The effects of change of the modulus, and hence the weighting of the phase [18] due to the effects listed below are now investigated:

(a) primary reflections,
(b) secondary reflections and
(c) filtering effects of the pipe.

In Fig. 8, the various components of the modulus of the CSD are plotted corresponding to the phase in Fig. 7a. Fig. 8a shows the modulus of the CSD with effects (a), (b) and (c) included. The effects due to the reflections are evident at low frequencies, and the attenuation in the modulus as frequency increases due to the damping in the pipe

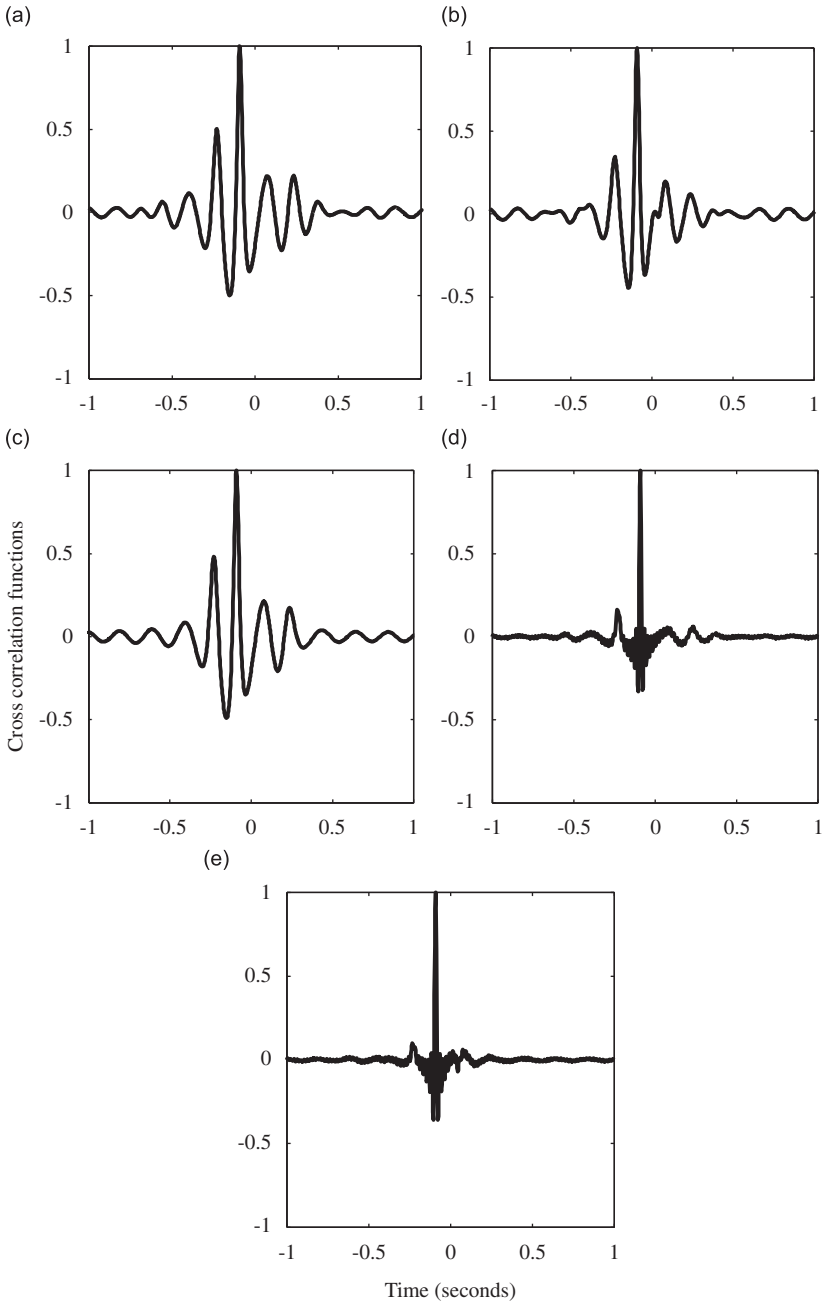

Fig. 9. Cross-correlation functions corresponding to the cross-spectra in Figs. 8 and 7(a) (normalised to the maximum value).

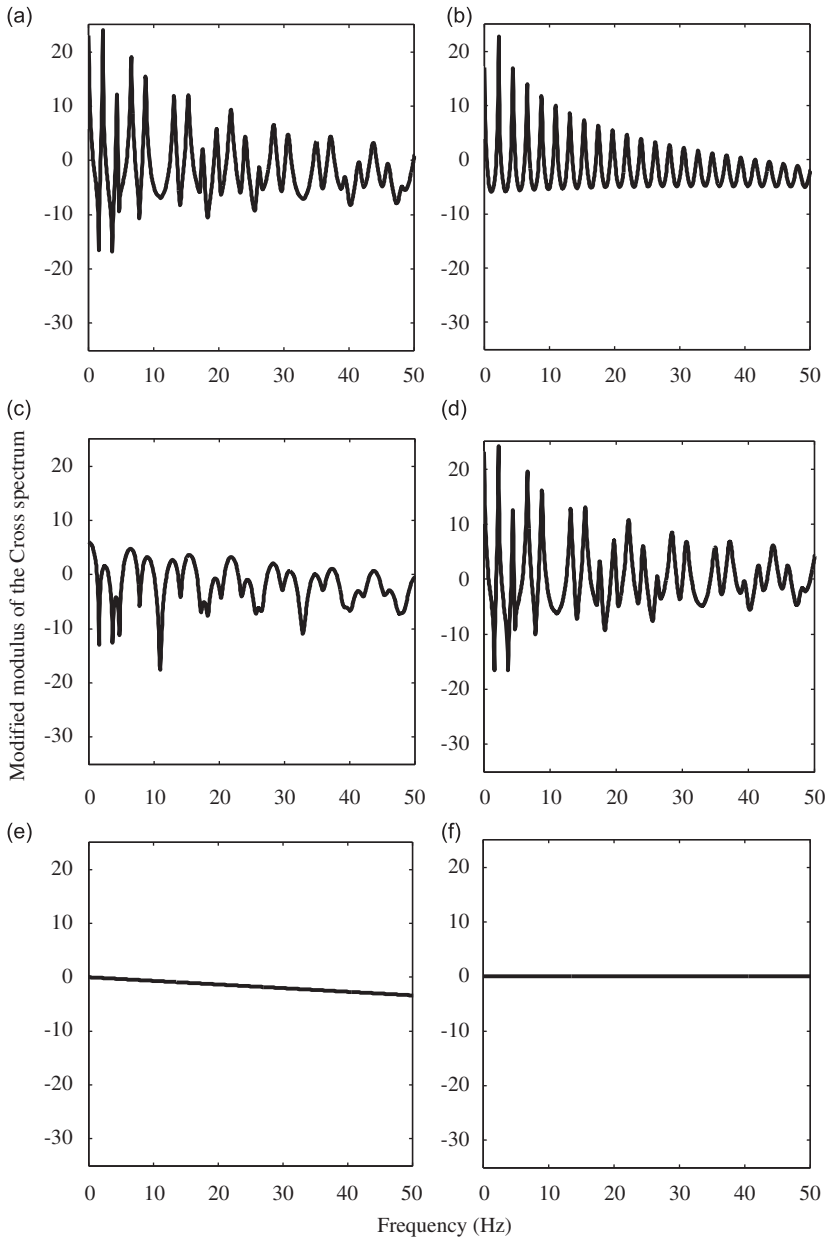

Fig. 10. Modified modulus of the cross-spectrum of the pressure signals corresponding to the phase spectrum in Fig. 7(b); $\eta = 0.022$, $d_1 = 76.7$ m, $d_2 = 32.8$ m, $c = 479\,\mathrm{ms}^{-1}$, $l_1 = l_2 = 0$, $r_1 = r_2 = 1$. (a) BCC, (b) primary reflections removed, (c) secondary reflections removed, (d) filtering effect of pipe removed, (e) primary and secondary reflections removed, (f) divided by the modulus of the cross-spectrum.

is also evident. Figs. 8b and c show the modulus of the CSD with primary and secondary reflections removed, respectively, and Fig. 8d shows the modulus with the pipe filtering effect removed ($C(\omega)$ in Eq. (13)). Finally, Fig. 8e shows the modulus with all the effects removed as it would be with the GCC PHAT. Fig. 9a–e shows the cross-correlation functions corresponding to the moduli given in Fig. 8a–e and the phase spectrum given in Fig. 7a.

Examining Fig. 9 it is clear that removal of the filtering effects of the pipe is the dominant factor in the GCC PHAT for the highly damped pipe. This is evident by comparing Fig. 9d and e where it can be seen that there is little difference between the two cross-correlation functions and the peaks due to the reflections are largely suppressed.

Figs. 10 and 11 give the corresponding graphs for the moduli and cross-correlation functions for the same system but with light damping, $\eta = 0.022$. The corresponding phase spectrum is plotted in Fig. 7b. It is evident

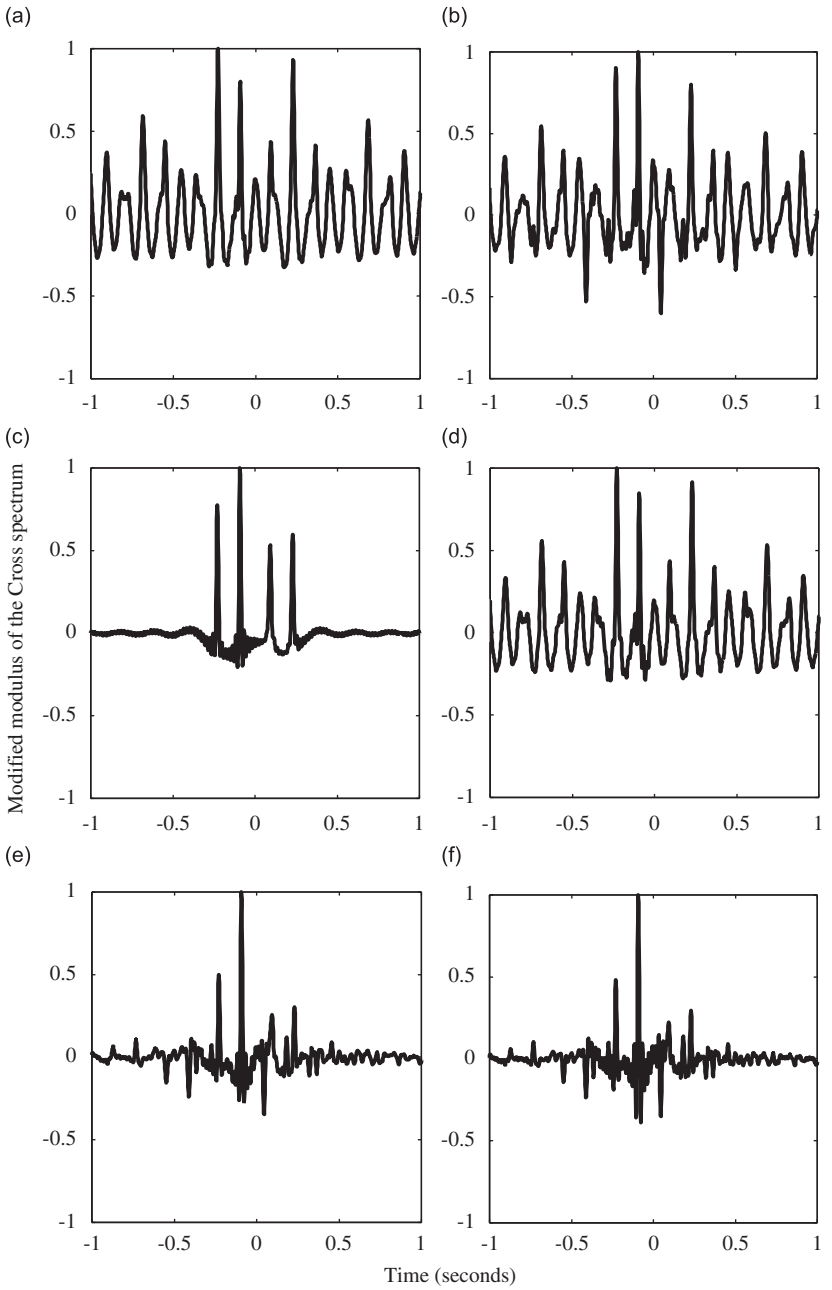

Fig. 11. Corresponding cross-correlation functions to the cross-spectra in Figs. 10 and 7b (normalised to the maximum value).

in this case that it is the primary and secondary reflections, rather than the low-pass filtering effect of the pipe that governs the suppression of the additional peaks by the GCC PHAT. This is because the filtering effect of the pipe is weak over the frequency bandwidth for which the analysis is conducted, and this is due to the light damping in the pipe and hence low wave attenuation.

5. Experimental results

The BCC and PHAT time delay estimators discussed in this paper were tested on experimental data measured at a specially constructed leak-detection facility located at a National Research Council site in Canada, a plan of which is shown

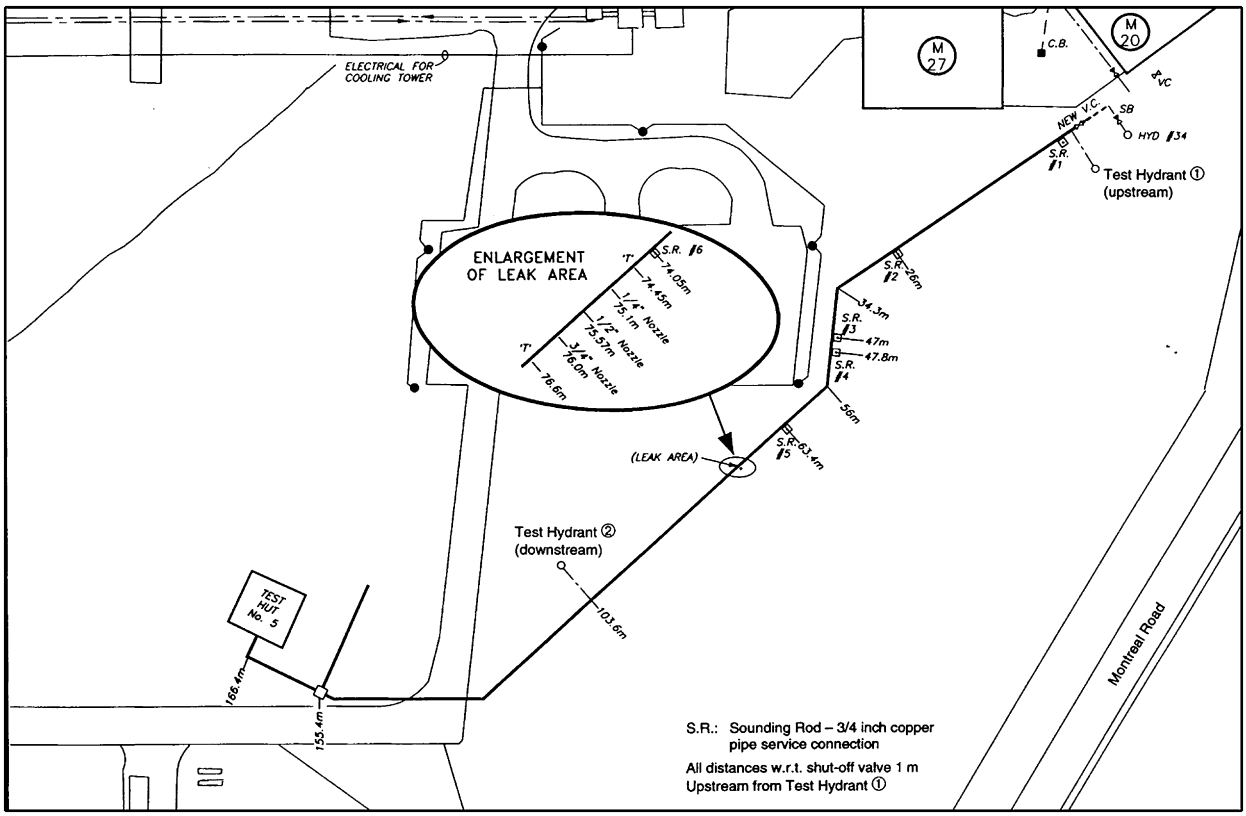

Fig. 12. Plan view of the experimental leak detection facility at the NRC, Canada [5].

in Fig. 12. The description of the test site and measurement procedures are detailed in Ref. [5]. Noise from a leaky joint was measured using hydrophones. Photographs showing the risers and hydrants connected to the main buried pipe are shown in Fig. 13a and b. The lengths of the riser upstream and downstream of the leak were 3.2 and 3.7 m, respectively. The distance between the two risers was 102.6 m, and the distance of the upstream riser from the leak was 73.5 m. Thus, in the simulations of the cross-correlation functions presented in this section (as in the previous sections), the distance d_1 was taken to be 78.5 m and the distance d_2 was 32.8 m. It was also assumed that there were perfectly reflecting terminations at the sensor positions, i.e. $l_1 = l_2 = 0$; $r_1 = r_2 = 1$.

In the experiment, the hydrophone-measured signals were each passed through an anti-aliasing filter with the cut-off frequency set at 200 Hz and sampled at a frequency of 500 samples/s. The time series were of 66-s duration.

The BCC calculated from the experimental data is shown in Fig. 14a. The corresponding simulation is shown in Fig. 14b. In the simulations, the damping in the pipe was adjusted to a value of 0.043, as this gave the best fit to the experimental results. Although the pipe system at the test-site was quite complicated in that there were bends and valves etc, the correlation predictions obtained using the relatively simple model described in Section 3 are in good agreement with the experimentally measured correlation function. The degree of agreement between prediction and experiment makes clear that the additional peaks in the cross-correlation function were due to reflections in the pipe.

The GCC PHAT was also calculated from the measured data and this is shown in Fig. 14c and the corresponding simulation in Fig. 14d. The removal of spurious reflection-related peaks by the use of this correlator can clearly be seen. The time delay due to the leak is now much more discernible.

6. Conclusions

The effect of reflections on the correlation technique for leak detection in plastic water pipes has been investigated. A model was developed of the correlation function including the pipe dynamics and the reflections due to discontinuities in the pipe.

It has been shown that, when reflections occur, in addition to the main peak in the BCC corresponding to the true time delay resulting from the propagating leak signals, there are several other spurious peaks. The phase of the CSD is governed

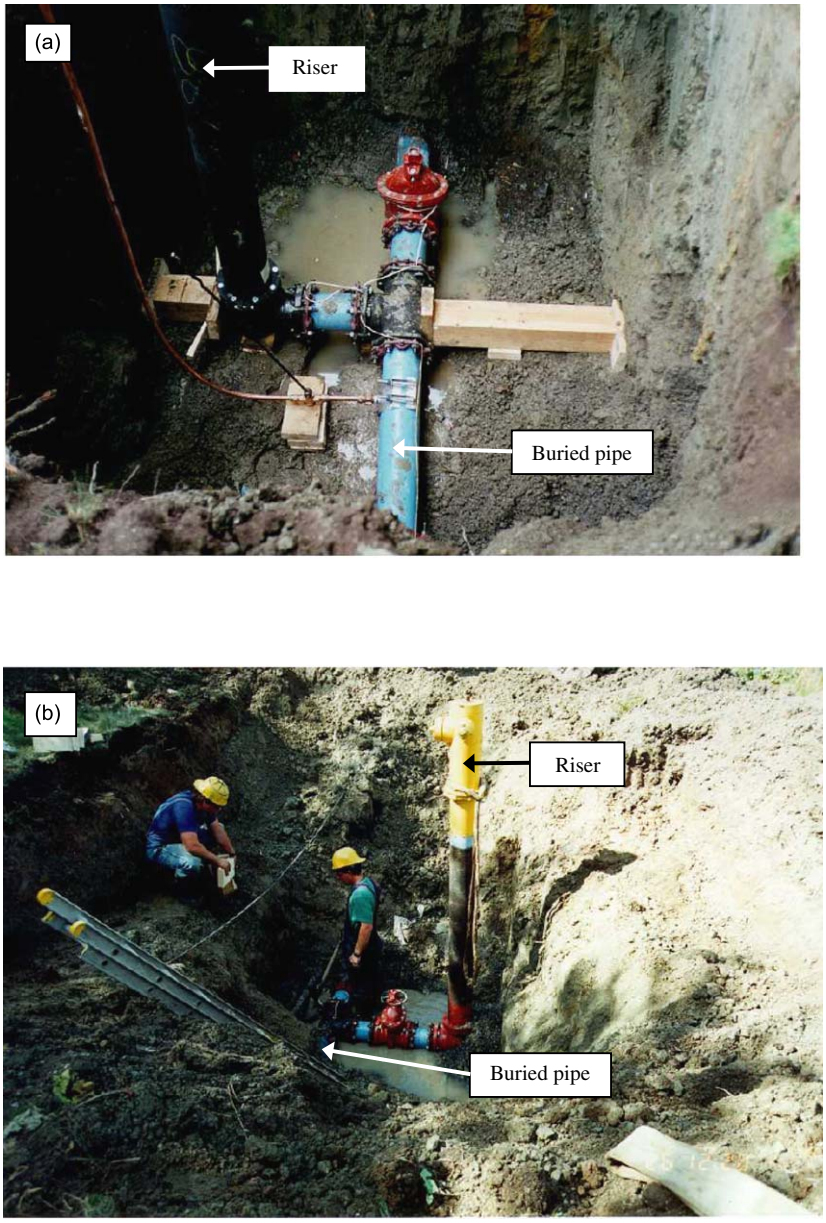

Fig. 13. (a) Upstream and (b) downstream fire hydrants of the test facility shown in Fig. 12 before reinstatement [5].

by the primary propagating/reflected waves and the time difference between the leak noise arrival at the two sensors. The primary and secondary reflections also have an effect on the modulus of the CSD as does the filtering effect of the pipe due to the attenuation of the leak noise signal because of damping in the pipe-wall. The individual effects of the primary reflections, secondary reflections and filtering effect of the pipe on the cross-correlation function have been investigated and quantified. It has been shown that if the pipe has low damping or the distance from the sensors to the leak is small then the reflections have a major influence on the cross-correlation function; if the damping is large or the distance from the sensors to the leak is large then the filtering properties of the pipe have a much greater influence on the cross-correlation function.

The theoretical predictions have been compared to hydrophone-measured data from actual water pipes, and it has been clearly shown that the additional peaks in the BCC are due to reflections due to discontinuities in the pipe. Moreover, it has been shown that by removing the effects of the reflections and the filtering properties of the pipe from the modulus of the CSD, the additional peaks due to the reflections can be largely removed from the cross-correlation function.

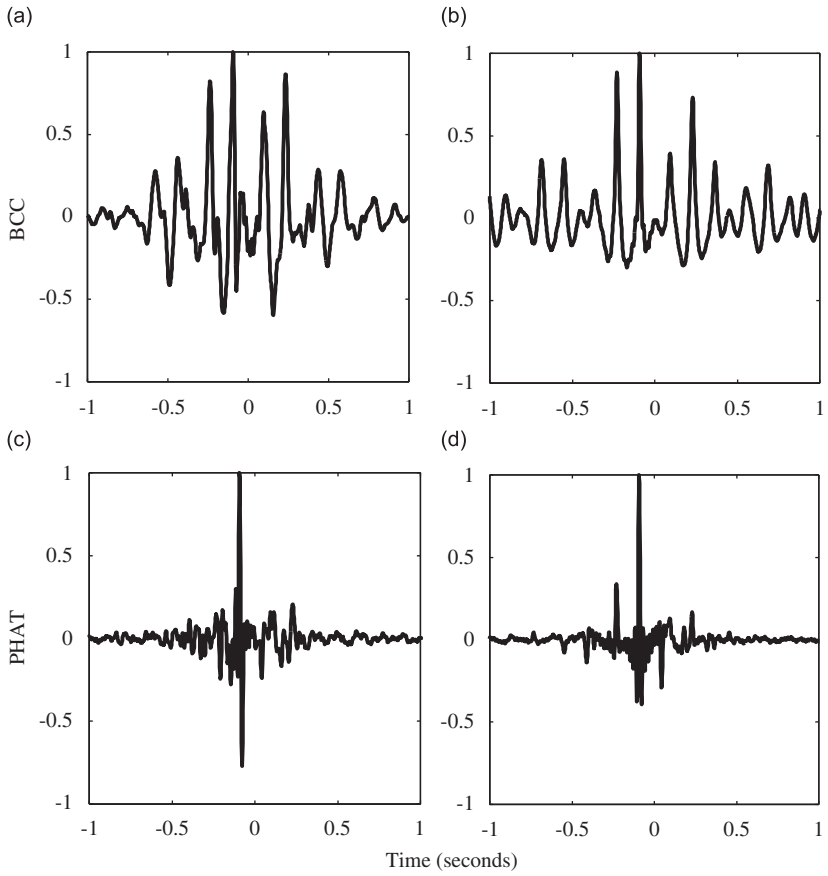

Fig. 14. Comparison between predictions and experimental results: (a) BCC experiment; (b) BCC simulation; (c) PHAT experiment; and (d) PHAT simulation. In both the simulations and the experiments the bandwidth was set to 5–50 Hz. In the simulations $\eta = 0.043$, $d_1 = 76.7$ m, $d_1 = 76.7$ m, $d_2 = 32.8$ m, $c = 479\,\mathrm{ms}^{-1}$, $l_1 = l_2 = 0$, $r_1 = r_2 = 1$. The cross correlation functions are normalised to their maximum values.

Acknowledgements

The authors gratefully acknowledge the support of the EPSRC under Grant GR/R13937/01 and Osama Hunaidi from the National Research Council of Canada who provided the test data.

References

[1] M. Fantozzi, G.D. Chirico, E. Fontana, F. Tonolini, Leak inspection on water pipelines by acoustic emission with cross-correlation method, *Annual Conference Proceeding, American Water Works Association, Engineering and Operations*, San Antonio, Texas, USA, 1993.
[2] H.V. Fuchs, R. Riehle, Ten years of experience with leak detection by acoustic signal analysis, *Applied Acoustics* 33 (1) (1991) 1–19.
[3] D.A. Liston, J.D. Liston, Leak detection techniques, *Journal of the New England Water Works Association* 106 (2) (1992) 103–108.
[4] O. Hunaidi, W.T. Chu, Acoustical characteristics of leak signals in plastic water distribution pipes, *Applied Acoustics* 58 (3) (1999) 235–254.
[5] O. Hunaidi, W. Chu, A. Wang, W. Guan, Detecting leaks in plastic pipes, *Journal of the American Water Works Association* 92 (2) (2000) 82–94.
[6] Y. Gao, M.J. Brennan, P.F. Joseph, J.M. Muggleton, O. Hunaidi, A model of the correlation function of leak noise in buried plastic pipes, *Journal of Sound and Vibration* 277 (1–2) (2004) 133–148.
[7] Y. Gao, M.J. Brennan, P.F. Joseph, A comparison of time delay estimators for the detection of leak noise signals in plastic water distribution pipes, *Journal of Sound and Vibration* 292 (2006) 552–570.
[8] C.H. Knapp, G.C. Carter, The generalised correlation method for estimation of time delay, *IEEE Transactions on Acoustics, Speech, and Signal Processing* 24 (4) (1976) 320–327.
[9] I. Al-Shidhani, S.B.M. Beck, W.J. Staszewski, Leak monitoring in pipeline networks using wavelet analysis, *Key Engineering Materials* 245–246 (2003) 51–58.
[10] Y. Gao, M.J. Brennan, P.F. Joseph, J.M. Muggleton, O. Hunaidi, On the selection of acoustic/vibration sensors for leak detection in plastic water pipes, *Journal of Sound and Vibration* 283 (3–5) (2005) 927–941.
[11] J.A. Fox, *Transient Flow in Pipes, Open Channels and Sewers*, Ellis Horwood, Chichester, 1989.
[12] A.R.D. Thorley, *Fluid Transients in Pipeline Systems*, D.&L. George Ltd., Hertfordshire, England, 1991.
[13] D.L. Margolis, W.C. Yang, Bond graph models for fluid networks using modal approximation, *Journal of Dynamics Systems, Measurement, and Control, Transactions of ASME* 107 (1985) 169–175.
[14] W.C. Yang, D.L. Margolis, Signal shaping of fluid transmission lines using parallel branching, *Journal of Dynamics Systems, Measurement, and Control, Transactions of ASME* 108 (1986) 296–305.

[15] D.M. Auslander, *Analysis of Network of Wavelike Transmission Elements*, Massachusetts Institute of Technology, USA, 1966.
[16] D.M. Auslander, Distributed system simulation with bilateral delay-line methods, *Journal of Basic Engineering, Transactions of ASME* (1968) 195–200.
[17] S.B.M. Beck, H. Haider, R.F. Boucher, Transmission line modelling of simulated drill strings undergoing water-hammer, *Journal of Mechanical Engineering Science, Proceedings of the Institution of Mechanical Engineers* 209 (C6) (1995) 419–427.
[18] M.J. Brennan, Y. Gao, P.F. Joseph, On the relationship between time and frequency domain methods in time for leak detection in plastic water pipes, *Journal of Sound and Vibration* 304 (1–2) (2007) 213–223.
[19] J.M. Muggleton, M.J. Brennan, P.W. Linford, Axisymmetric wave propagation in fluid-filled pipes: measurements in in-vacuo and buried pipes, *Journal of Sound and Vibration* 270 (2004) 171–190.